Nanoscale Res Lett (2009) 4:1428–1433
DOI 10.1007/s11671-009-9415-6

NANO EXPRESS

Fabrication of Anti-human Cardiac Troponin I Immunogold Nanorods for Sensing Acute Myocardial Damage

Z. R. Guo · C. R. Gu · X. Fan · Z. P. Bian · H. F. Wu · D. Yang · N. Gu · J. N. Zhang

Received: 1 July 2009 / Accepted: 9 August 2009 / Published online: 21 August 2009

Abstract A facile, rapid, solution-phase method of detecting human cardiac troponin I for sensing myocardial damage has been described using gold nanorods-based biosensors. The sensing is demonstrated by the distinct change of the longitudinal surface plasmon resonance wavelength of the gold nanorods to specific antibody–antigen binding events. For a higher sensitivity, the aspect ratio of gold nanorods is increased up to ca 5.5 by simply adding small amount of HCl in seed-mediated growth solution. Experimental results show that the detecting limit of the present method is 10 ng/mL. Contrast tests reveal that these gold nanorods-based plasmonic biosensors hold much higher sensitivity than that of conventionally spherical gold nanoparticles.

Keywords Gold nanorod · Biosensor · Surface modification · Cardiac troponin I

C. R. Gu is the co-first author.

Electronic supplementary material The online version of this article (doi:10.1007/s11671-009-9415-6) contains supplementary material, which is available to authorized users.

Z. R. Guo · C. R. Gu · Z. P. Bian · H. F. Wu · D. Yang · J. N. Zhang (✉)
The Research Institute of Cardiovascular Disease, The First Affiliated Hospital of Nanjing Medical University, 210029 Nanjing, China
e-mail: jinanzh506@yahoo.com

Z. R. Guo · X. Fan · N. Gu
State Key Laboratory of Bioelectronics and Jiangsu Laboratory for Biomaterials and Devices, Southeast University, 210029 Nanjing, China

Introduction

Cardiac troponin I (cTnI) is a protein subunit of cardiac troponin complex. During the myocardial damage process, the troponin complex is broken up, and the individual protein components including cTnI are released into the bloodstream [1]. Early detection of cTnI in the serum of patients with a higher risk of acute myocardial infarction can decrease the danger of death from heart attack. Because of high tissue specificity that ensuring an accurate assay, cTnI has been considered as the "gold standard" of cardiac marker for clinic diagnosis of acute myocardial damage [2–4]. Currently, most cTnI detections are based on the traditional enzyme linked immunosorbent assay (ELISA) methods. For a typical ELISA process, a capture anti-cTnI antibody against cTnI is firstly immobilized onto the surface of plastic well, followed by adding a patient sample containing cTnI for binding the capture anti-cTnI antibody. Then an enzyme labeled detector anti-cTnI antibody is allowed to bind with the immobilized cTnI. In each step mentioned above, quite a few wash cycles are necessary in order to remove the unbound antibody or antigen from the well. Finally, enzymatic substrate is added, and cTnI is detected by an enzyme-dependent color-change reaction. The entire ELISA process can usually take several hours to days to accomplish, which is labor-intensive and time-consuming. To overcome these limitations, it is of significance to develop a convenient, rapid and homogeneous immunoassays strategy for detecting cTnI events.

In recent years, biomedical research has received a large advancement, which greatly benefit from the development of nanomaterials [5–7]. Among these nanomaterials, gold nanoparticles (NPs) hold unique optical properties called localized surface plasmon resonance (LSPR) arising from

oscillation of the free electrons in the gold, good biosafety and facile surface modification, enabling them quite suitable nanoscale platforms for biosensing or antibody–antigen immunoassay [8]. In general, the label-free sensing using gold NPs can be achieved by analyte-mediated gold NPs aggregation. This concept is that the surface of the gold NPs needs to be modified with recognition molecules that specifically bind the analyte of interest. The recognition molecules-modified gold NPs will be brought very close to each other by recognition molecule-target molecular conjugation after adding the analyte solution, which brings on the coupling of plasmon resonances from adjacent NPs. As a result, the SPR band(s) of aggregated gold NPs will be broadened and red-shifted as a function of the amount of analyte. These changes can be recorded on a conventional UV–visible spectrophotometer [9]. As a face-centered cubic metal with intrinsically high symmetry, the most common and easily obtained shape of gold NPs is a spherical one. For this main reason, spherical gold NPs are involved in most of the exiting works utilizing gold NPs aggregation effects to sense specific target binding events so far. Recently, both experimental and computational studies have revealed that the shape of gold NPs plays a key role in determining their optical properties [8, 10–12]. In particular, gold NPs with elongated shape called nanorods (NRs) have attracted much attention, because their highly anisotropic shape exhibits specially optical properties that are much different from commonly spherical ones [13]. For instance, gold NRs show two distinct LSPR bands owing to the transverse and the longitudinal oscillation of the electrons respectively, one at short wavelength about 510 nm and the other at long wavelength beyond 600 nm, whereas spherical gold NPs displays only one band around 520 nm. In terms of LSPR sensing, there are several advantages to gold NRs compared to spherical NPs. First of all, the longitudinal SPR band of gold NRs has a higher sensitivity to the changes of the local dielectric surroundings, including solvent, adsorbed molecules and the aggregate state, when compared to similar-sized spherical NPs [14–16]. Since the longitudinal and transverse LSPR bands of gold NRs are basically independent of each other, one can use the changes of the longitudinal SPR band for more sensitive detection of target molecules. Secondly, it is also observed that this sensitivity of longitudinal band increases with higher aspect ratio (length divided by width, denoted as AR), leading to an improved detection sensitivity [17, 18]. In addition, increasing the AR of gold NRs can easily tailor the longitudinal SPR band from the visible to the near infrared (NIR) region (700–1,000 nm), which is a transparent window for hemoglobin and facilitate the detection of whole blood samples [19]. Thirdly, because spherical shape has the smallest surface area relative to objects of other shapes (when the volume is fixed), gold NRs give a much larger surface area compared with spherical ones for adsorption of protein. Thanks to the efforts of many research groups, gold NRs can be synthesized routinely with high monodispersity at present time, which is an essential factor for using gold NR as LSPR sensors.

In this letter, we describe a convenient and rapid method for human cTnI detection in solution using anti-human cTnI immunogold NRs. The sensing was based on changes of longitudinal LSPR band induced by specific anti-h-cTnI antibody-h-cTnI binding events. To our knowledge, it is the first report of taking advantage of gold NRs for sensing h-cTnI. In order to improve the sensitivity, gold NRs with a higher AR ca. 5.5 are fabricated successfully by adding small amount of HCl in the growth solution through a modified seed-mediated approach. The detection limit of the present method is 10 ng/mL, which exhibits much higher sensitivity of detecting h-cTnI events than that of spherical gold NPs.

Experimental Sections

Materials

Cetyltrimethylammonium bromide (CTAB, 99%, Cat No: H6269) and Poly(styrenesulfonate) (PSS, Mw 70,000) were purchased from Sigma. Hydrogen tetrachloroauric acid ($HAuCl_4{\cdot}4H_2O$, 99%), hydrochloric acid (HCl), sliver nitrate, sodium borohydride ($NaBH_4$, 96%) and L-ascorbic acid (AA) were all purchased from Shanghai Chemical Reagent Co. Ltd (China). Millipore-quality water (18.18 MΩ/cm) was used throughout the experiments. cTnI from human myocardium muscle and the monoclonal anti-human cTnI antibodies used in the experiment were obtained from Research Institute of Cardiovascular Disease of First Affiliated Hospital of Nanjing Medical University.

Fabrication of Monodisperse Gold NRs

Gold NRs were fabricated based on a seed mediated, CTAB-assisted growth procedure by Nikoobakht et al. [20] with some modifications. Gold seed solution was prepared first by adding 0.6 mL of ice-cold solution of 10 mM $NaBH_4$ to 10 mL of 0.25 mM $HAuCl_4$ prepared in 0.1 M CTAB solution, under vigorous stirring for 2 min. The yellow color changed immediately to brown, indicating the formation of gold seeds. These seeds were aged for 2 h in order to allow the hydrolysis of unreacted $NaBH_4$.The growth procedure was scaled up to obtain a 100 mL dispersion of the gold NRs. Briefly, the solutions were added to a 250 mL conical flask, in the following order: 100 mL

of 0.1 M CTAB solution, 1.0 mL of 10 mM silver nitrate solution, 2 mL of 25 mM aqueous $HAuCl_4$ and 0.4 mL of 1 M HCl solution. To this was added 0.70 mL of 0.0788 M AA as reducing agent, and the mixture was homogenized by stirring gently. Finally, 120 μL of seed solution was added, and the whole solution was left undisturbed overnight (14–16 h).

PSS Coating

Typically, 10 mL of as-fabricated gold NRs was centrifuged at 13,000 g/min for 20 min, the supernatant was discarded, and the precipitate was redispersed in 5 mL of Milli-Q water. Subsequently, it was added dropwise to 1 mL of PSS (2.5 mg/L,) aqueous solution under vigorous stirring. After adding PSS solution, the mixture was kept undisturbed for 0.5 h. Then, it was centrifuged twice at 12,500 g/min to remove excess polyelectrolyte and dispersed in 5 mL of Tris buffer (pH = 8.2).

Conjugation of Anti-h-cTnI Antibody with PSS-capped Gold NRs

The PSS-capped gold NRs were mixed with excess amount of anti-h-cTnI solution (50 μg/mL in Tris buffer) for 30 min under magnetic stirring. The mixture was centrifuged in order to remove unbinding antibodies and redispersed into Tris buffer. Finally, these antibody conjugated gold NRs were store at 4 °C for further utilization.

Binding of h-cTnI to Anti-h-cTnI Antibody Conjugated Gold NRs

In each experiment, 1.0 mL of anti-cTnI antibody conjugated gold NRs was added to a fixed amount (1, 10, 100, 200, 400, 500 ng) of h-cTnI under vortex mixing. The resultant mixture was incubated for 15 min before recording with 2802S (UNICO) spectrophotometer.

Characterization

Transmission electron microscopy (TEM) images were taken with a JEM-2000EX (JEOL) transmission electron microscope operated at 120 kV. The samples were prepared by dropping the dispersion of gold products onto the carbon-coated copper grid and dried in ambience. UV–vis–NIR spectra were recorded on a 2802S (UNICO) spectrophotometer in the 300–1,100 nm range. Fourier transform infrared (FTIR) spectra were measured on a Magna FTIR-750 (Nicolet) spectrometer, and the vacuum-dried sample was made in the form of a KBr pellet.

Results and Discussion

Fabrication, Surface Functionalization and Characterization of Gold NRs

According to the seed mediated, CTAB-assisted growth approach by Nikoobakht et al. [20], the AR of gold NR can be increased up to 4.5 by adjusting the amount of silver. Thus, our first aim is to fabricate gold NRs with AR 4.5 for higher detection sensitivity. However, we could only obtain gold NRs with AR 3.5 when adopting the same recipe by Nikoobakht et al. (Fig. 1). Very recently, Smith and Korgel demonstrated that iodide impurity at ppm concentrations present in CTAB prevents gold NRs formation [21]. It has been found that iodide tends to adsorb onto the {111} facets—the end surface of the gold NRs—and slows the gold deposition rate on these facets, which results in either gold NRs with lower AR or even spherical gold NPs [21]. To overcome this problem, we add a small amount of HCl solution to the growth solution for decreasing the whole reduction rate, because AA has a much weaker reducing power in strong acidic solution than in weak acidic solution [13, 22]. By doing this, we presume that the growth rate of the lateral surfaces of gold NRs, such as {110} facets, could fall down correspondingly and facilitate the formation of gold NRs with a higher AR. Figure 2 shows the effect of adding identical growth solutions to 0–0.8 mL of 1 M HCl solution. It can be seen that by increasing the HCl amount, the longitudinal LSPR band red shifts dramatically from 710 up to 856 nm. Correspondingly, the average AR of gold NRs rises from 3.5 to 5.5 by TEM observation. In all the samples, the fraction of NR-shaped gold particles consisting of spheres and cubes is less than 3%. In this research, the as-fabricated gold NRs with AR 5.5 have been chosen to use in the whole

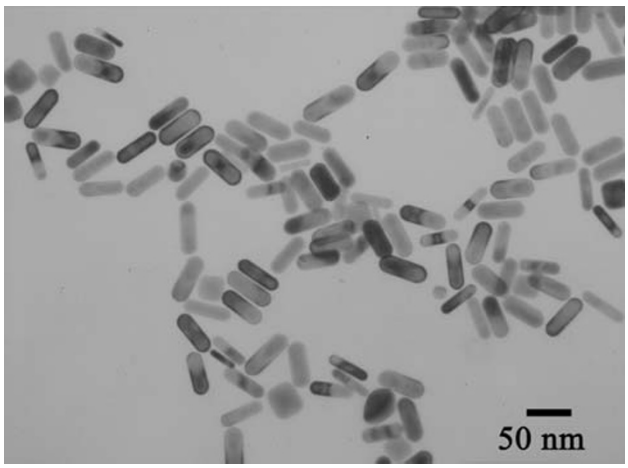

Fig. 1 TEM image of gold NRs fabricated without adding HCl to the growth solution

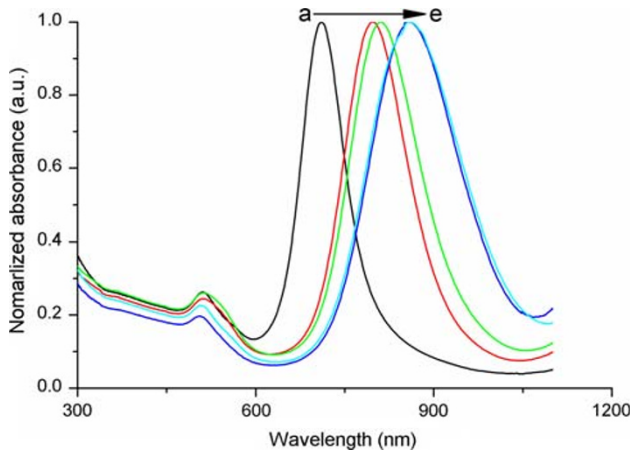

Fig. 2 Effect of the HCl concentration on the UV–vis–NIR absorption spectra of gold NRs. The longitudinal SPR band red shifts by increasing the amount of 1 M HCl solution added: *a* 0 mL; *b* 0.1 mL; *c* 0.2 mL; *d* 0.4 mL; *e* 0.8 mL

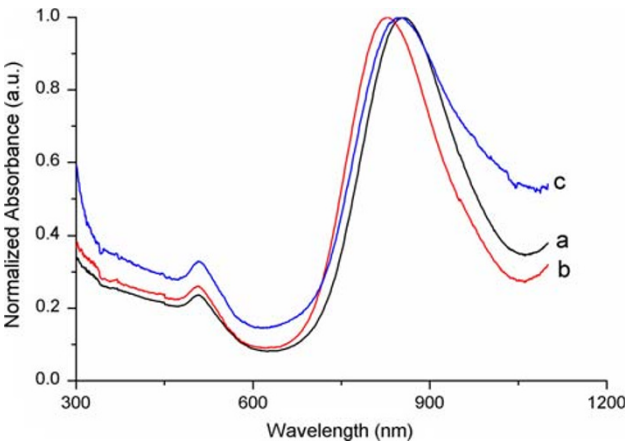

Fig. 4 UV–vis–NIR absorption spectra of gold NRs at different stages of surface functionalization: *a* as-fabricated gold NRs with average AR 5.5; *b* PSS-coated gold NRs and *c* anti-h-cTnI antibody conjugated gold NRs

experiments. The crude gold NRs are capped by CTAB bilayers and are positively charged on the surface [22]. Although there are some publications describe that the washed CTAB-capped gold NRs are found to be nontoxic and able to conjugate antibody protein directly [23, 24], our tests do reveal that the CTAB on the gold NRs cause the denaturation and sedimentation of anti-h-cTnI antibodies. To passivate the cytotoxicity of CTAB, anionic polyelectrolyte PSS has been coated on the surface of gold NRs by electrostatic interaction before antibody conjugation. The conjugation of antibody on the PSS-coated gold NRs possibly lies in two interactions illustrated in Fig. 3: (1).The electrostatic interaction between the negatively charged PSS and the positively charged segment of the antibody; (2). The hydrophobic interaction between PSS and the antibody [25, 26]. Figure 4 shows the absorption spectra of gold NRs before and after PSS coating and subsequent antibody conjugation. The longitudinal LSPR absorption maximum has a 28 nm blue shift after PSS

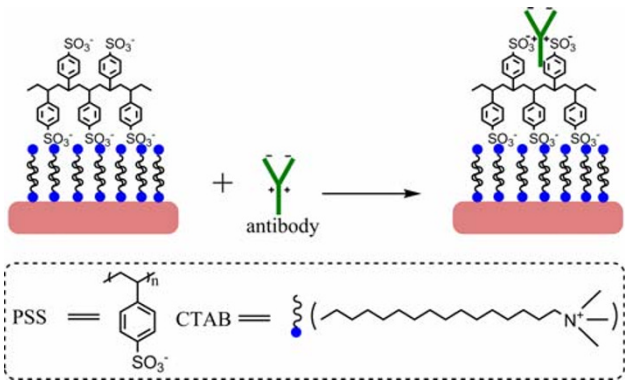

Fig. 3 Schematic illustration of conjugation of PSS-coated gold NRs with anti-h-cTnI antibody

coating (Fig. 4b). After anti-h-cTnI antibody conjugating to the PSS layer, there is an 18 nm red shift of the longitudinal LSPR absorption maximum (Fig. 4c). No shift in the absorption maximum of the transverse LSPR is observed during the whole process, indicating that the longitudinal SPR of gold NRs is extremely sensitive to the changes of the local dielectric surrounding. FTIR measurements have been performed on the CTAB gold NRs before and after PSS coating and subsequent anti-h-cTnI antibody conjugation. It can be seen clearly that sharp characteristic peaks of different functional groups emerge after the conjugation of antibody on the PSS-coated gold NRs, which confirms the formation of NR-bound antibody composites (Supplementary material, Fig. S1). TEM images have been recorded for the CTAB-capped gold NRs before (Fig. 5a) and after surface modification by PSS (Fig. 5b) and subsequent anti-h-cTnI antibody (Fig. 5c) in turn. Both CTAB-capped gold NRs and PSS-coated gold NRs can be clearly seen from the TEM images (Fig. 5a,b). However, the image of gold NRs after antibody conjugation is quite obscure (Fig. 5c), due to the large size and nonconductibility of the antibodies.

Detection of h-cTnI Using Anti-h-cTnI Antibody Conjugated Gold NRs in Solution

Figure 6 reveals the changes in the absorbance of the anti-h-cTnI antibody conjugated gold NRs solution after the addition of h-cTnI at different concentrations. It can be seen the longitudinal SPR band is continuously red-shifted (from 846 to 866 nm) and decreases in intensity distinctly due to the antibody–antigen recognition event, when increasing the concentration of h-cTnI from 1 to 200 ng/mL. The spectra results indicate that the specific detection of h-cTnI

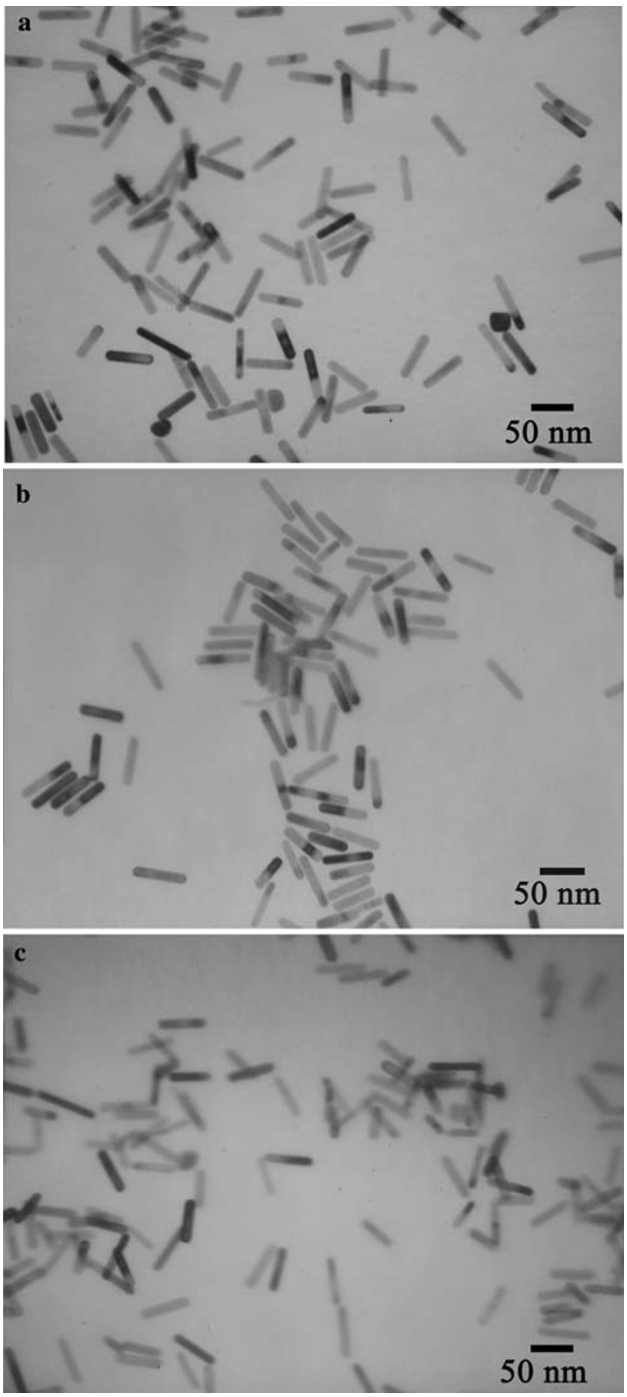

Fig. 5 TEM images of gold NRs with different surface coating: **a** as-synthesized, CTAB-capped gold NRs with average AR 5.5, **b** after PSS coating and subsequent, **c** anti-h-cTnI antibody conjugation

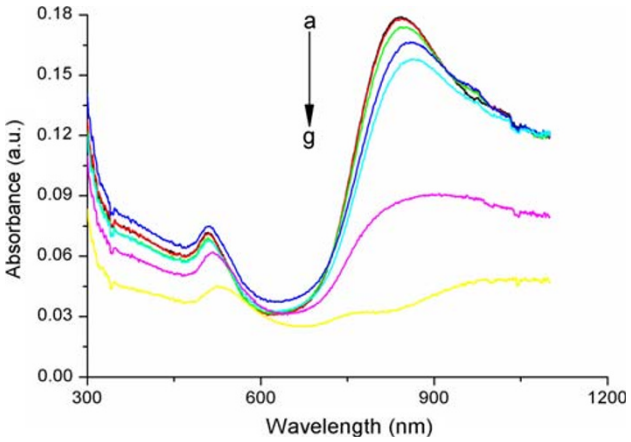

Fig. 6 UV–vis–NIR absorbance spectra for *a* gold NRs after conjugation of anti-cTnI antibody, and *b–g* the gold NRs conjugated with anti-h-cTnI antibody after treatment with h-cTnI (1, 10, 100, 200, 400 and 500 ng/mL in Tris buffer, respectively)

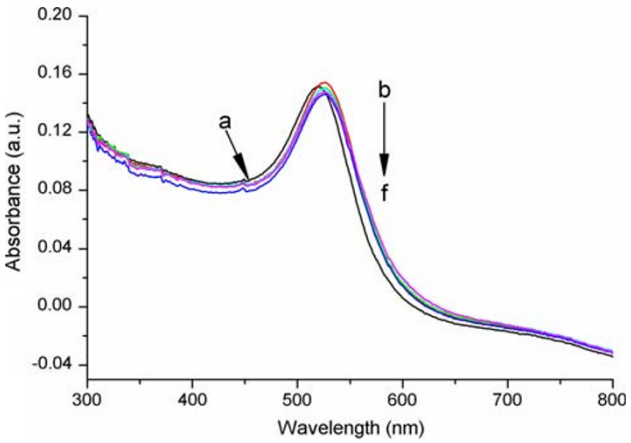

Fig. 7 UV–vis–NIR absorbance spectra for *a* uncapped spherical gold NPs, *b* spherical gold NPs after conjugation of anti-h-cTnI antibody and *c–f* the gold nanoparticles conjugated with anti-h-cTnI antibody after treatment with h-cTnI (1, 10, 100, 200 ng/mL in Tris buffer, respectively)

by these gold NR biosensors is achieved with a sensitivity of 10 ng/mL. Furthermore, broadening of the longitudinal band is also observed under high concentration of h-cTnI (>200 ng/ml), which might be due to the aggregation of gold NRs driven by the increasing specific binding events of anti-h-cTnI antibody and h-cTnI. To investigate the nonspecific adsorption of other proteins on the anti-h-cTnI antibody conjugated gold NRs, control experiment has been conducted by detecting goat IgG instead of h-cTnI, and longitudinal SPR band change is observed (Supplementary material, Fig. S2). These results confirm that the changes in longitudinal band of gold NRs arise from the specific recognition between anti-h-cTnI antibody and h-cTnI. Moreover, we have also used spherical, citrate-stabilized gold NPs with a diameter of 20 nm as platforms for sensing h-cTnI. The experimental results show that corresponding changes in the LSPR band are quite weak compared with that of gold NRs at the same detecting concentrations (Fig. 7), indicating that the gold NRs-based biosensors are more effective for detecting cTnI events.

Conclusions

In summary, we have described here a rapid and sensitive method of detecting human cTnI for sensing myocardial damage. This method is based on the changes of longitudinal SPR band of gold NRs induced by the anti-h-cTnI antibody-h-cTnI recognition events. For purpose of improving the detect sensitivity, the average AR of gold NRs is adjusted to 5.5 by adding a proper amount of HCl to the seed-mediated growth solution. The detection limit of the present method is 10 ng/mL. Contrast tests reveal clearly that these gold NRs-based biosensors are more sensitive for detecting cTnI events compared with that of spherical gold NPs. We are currently conducting studies for multiplex detection of the biomarkers of coronary syndrome by utilizing the AR dependence of the longitudinal LSPR wavelength of gold NRs.

Acknowledgments The authors gratefully acknowledge the support of the Medical Key Talent of Jiangsu Province (RC2007037) and the High-technology Platform of Jiangsu Province for Molecular Diagnosis and Biological Therapy of Critical Illness (XK200705). Dr. X. Z. Zhang would be greatly appreciated for technique assistance.

References

1. M.C. Fishbein, T. Wang, M. Matijasevic, L.S. Hong, F.S. Apple, Cardiovasc. Pathol. **12**, 65 (2003)
2. O.F. Layrtza, H. Nayer, M.J. Bill, L.J. Sokoll, Clin. Chim. Acta **337**, 173 (2003)
3. H. Zimmet, Heart Lung Circ. **12**, S90 (2003)
4. The Joint European Society of Cardiology/Am College of Cardiology Committee, J. Am. Coll. Cardiol. **36**, 959 (2000)
5. H. Yang, Y. Xia, Adv. Mater. **19**, 3085 (2007)
6. X. Wang, L. Yang, Z. Chen, D.M. Shin, CA Cancer J. Clin. **58**, 97 (2008)
7. M. De, P.S. Ghosh, V.M. Rotello, Adv. Mater. **20**, 1 (2008)
8. M. Hu, J. Chen, Z. Li, L. Au, G.V. Hartland, X. Li, M. Marqueze, Y. Xia, Chem. Soc. Rev. **35**, 1084 (2006)
9. N.L. Rosi, C.A. Mirkin, Chem. Rev. **105**, 1547 (2005)
10. L.M. Liz-Marzán, Langmuir **22**, 32 (2006)
11. C.J. Orendorff, T.K. Sau, C.J. Murphy, Small **2**, 636 (2006)
12. C. Noguez, J. Phys. Chem. C **111**, 3806 (2007)
13. C.J. Murphy, A.M. Gole, S.E. Hunyadi, C.J. Orendorff, Inorg. Chem. **45**, 7544 (2006)
14. A.D. McFarland, R.P. Van Duyne, Nano Lett. **3**, 1057 (2003)
15. H. Chen, X. Kou, Z. Yang, W. Ni, J. Wang, Langmuir **24**, 5233 (2008)
16. C.G. Wang, Y. Chen, T.T. Wang, Z.F. Ma, Z.M. Su, Chem. Mater. **19**, 5809 (2007)
17. K.S. Lee, M.A. El-Sayed, J. Phys. Chem. B **110**, 19220 (2006)
18. C.D. Chen, S.F. Cheng, L.K. Chau, C.R.C. Wang, Biosens. Bioelectron. **22**, 926 (2007)
19. P.K. Jain, I.H. El-Sayed, M.A. El-Sayed, Nano Today **2**, 18 (2007)
20. B. Nikoobakht, M.A. El-Sayed, Chem. Mater. **15**, 1957 (2003)
21. D.K. Smith, N.R. Miller, B.A. Korgel, doi: 10.1021/la900757s (2009)
22. C.J. Murphy, T.K. Sau, A.M. Gole, C.J. Orendorf, J. Gao, L. Gou, S.E. Hunyadi, T. Li, J. Phys. Chem. B **109**, 13857 (2005)
23. E.E. Connor, J. Mwamuka, A. Gole, C.J. Murphy, M.D. Wyatt, Small **1**, 325 (2005)
24. X. Liu, Q. Dai, L. Austin, J. Coutts, G. Knowles, J. Zou, H. Chen, Q. Huo, J. Am. Chem. Soc. **130**, 2780 (2008)
25. F. Caruso, K. Niikura, D.N. Furlong, Y. Okahata, Langmuir **13**, 3427 (1997)
26. H. Ai, M. Fang, S.A. Jones, Y.M. Lvov, Biomacromolecules **3**, 560 (2002)